

Article

Enhanced Oxygen Reduction Reaction of LSCF Cathode Material Added with NiO for IT-SOFC

Ahmad Zaki Mohamed Rosli¹, Nafisah Osman², Mahendra Rao Somalu³,
and Noorashrina A. Hamid^{1,*}

¹ School of Chemical Engineering, Engineering Campus, Universiti Sains Malaysia, 14300 Nibong Tebal Penang, Malaysia

² Faculty of Applied Sciences, Universiti Teknologi MARA, Kampus Arau, Cawangan Perlis, 02600 Arau, Perlis, Malaysia

³ Fuel Cell Institute, Universiti Kebangsaan Malaysia, UKM, 43600 Bangi, Selangor, Malaysia

*Email: chrina@usm.my (Corresponding author)

Abstract. $\text{La}_{0.6}\text{Sr}_{0.4}\text{Co}_{0.2}\text{Fe}_{0.8}\text{O}_{3-\delta}$ (LSCF) is one of the mixed ionic electronic conductors that could be feasibly used in an intermediate temperature solid oxide fuel cell (IT-SOFC). In this study, LSCF and NiO were prepared using a modified Pechini method and calcined at three different temperatures ranging from 600 °C to 900 °C. The prepared LSCF was added with 5% NiO (denoted as LSCF-NiO) as cathode material. The physical and electrical properties of the prepared cathode were investigated. X-ray diffraction data revealed that at calcination temperatures of 600 °C–900 °C, NiO and LSCF maintained their phases and conformed the cubic structure for NiO and orthorhombic structure for LSCF. The calcination temperature showed significant influence on the particle size of the prepared LSCF-NiO, as depicted by scanning electron microscopy (SEM), and all the powders reached a nanoscale size. The SEM cross section of LSCF-NiO layer on gadolinium-doped cerium electrolyte showed an acceptable percentage of cathode porosity and good adhesivity at cathode/electrolyte interface. Energy dispersive X-ray analysis further verified the purity of the samples. Brunauer–Emmett–Teller surface area analysis was conducted, and the results revealed a trend of decreased surface area with an increase in calcining temperature. At an operating temperature of 800 °C, the electrochemical impedance spectroscopic results showed that LSCF-NiO 800 had a low R_p of 0.07 $\Omega \text{ cm}^2$, and its E_a was found to be 159.5 kJ/mol, indicating that LSCF-NiO 800 is fit to be used as cathode material in IT-SOFC application.

Keywords: Cathode, LSCF-NiO, characterization, modified sol-gel method, IT- SOFC.

ENGINEERING JOURNAL Volume 26 Issue 9

Received 30 May 2022

Accepted 13 September 2022

Published 30 September 2022

Online at <https://engj.org/>

DOI:10.4186/ej.2022.26.9.11

1. Introduction

Fuel cell is a technology that converts chemical energy to electrical energy through redox reaction producing a clean by-product, which is usually is heat and water. Solid oxide fuel cell (SOFC) is a type of fuel cell that usually operates at high temperature (800 °C–1000 °C). SOFC is known for its high conversion efficiency, fuel flexibility, low emission, and relatively low cost. However, its high operating temperature causes long start-up times, material degradation, and high manufacturing and maintenance cost. Therefore, studies on lowering the operational temperature of SOFC from high to intermediate temperature (500 °C–800 °C) (IT-SOFC) have been receiving much attention in recent years. In SOFCs, the oxygen from the air is reduced to oxygen ions at the cathode to transfer through the electrolyte and react to the hydrogen fuel in the anode side to form water as a waste product. This oxygen reduction reaction (ORR) is vital in determining how much electrical energy is being produced in the system. The transfer of oxygen ions is restricted to the polarization resistance of the cathode itself. Therefore, lowering the resistance to improve the performance of SOFC at low temperature is desirable.

One of the choices to enhance SOFC performance at intermediate temperature is to utilize mixed ionic electronic conductor (MIEC) cathode. This cathode eases the ORR and assimilation in the electrolyte. A previous study focused on comparing the performance of traditional cathode and MIEC at intermediate temperature and concluded that MIEC possesses all the required characteristics to be used at the temperature range of 500 °C–800 °C [1]. Lanthanum Strontium Cobalt Ferrite (LSCF) is one of the state-of-art MIECs being used in IT-SOFC due to its high electrical conductivity and fast surface exchange kinetics [2]. LSCF is usually prepared in composite form with different materials that alter its surface and material properties to further improve its performance [3]. Composite cathodes containing LSCF usually exhibit lower polarization resistance than pure LSCF, hence better performance [4]. In the SOFC field, surface morphology and particle size are the most important factors that determine the ORR of the cathode. Smaller particle size is very much desirable because it causes larger specific surface area (SSA), increased triple boundary phase, and enhanced ORR and improves the performance [5]. Smaller particle size due to the addition of other materials could cause an increase in SSA, leading to enlarged triple-phase boundary (TPB).

Previous researchers have added metal oxides, such as CaO [6], PbO [7], MgO [8] and CuO [2, 9, 10] reported improvement on the surface morphology of the cathode samples. Fine deposition of CaO particles on the LSCF surface was reported, and its infiltration caused a smaller particle size of approximately 50 nm. Furthermore, a strong bonding between LSCF and CaO nanoparticles was reported by Zhang et al. in 2017 [6]. The addition of PbO and MgO also revealed small particles attached to large LSCF particles with a decent connection between

them and a random coverage of nanoparticles. No solid-state reactions were reported between phases, as shown in the partial enlargement of the boundary [7, 8]. LSCF-SDC-CuO was studied, and porous interlayer and homogeneous and fine grain size with 2 mol% of CuO give the lowest area specific resistance ($0.15 \Omega \text{ cm}^2$) were reported [2]. In addition, a strong interlayer bond and an enlarged TPB due to porous interlayer could facilitate ORR. Another study also reported a decrease in optimal calcination temperature, well-connected pores, particle distribution, reduction in grain size, and enhancement of electrocatalytic activity due to the presence of CuO [2]. Meanwhile, LSCF-CuO showed a decent contact area with no delamination after sintering [9]. The same researcher reported that high sintering temperature caused enlarged particle size in bulk form; therefore, decreased cathodic performance could be expected due to the large particle size [10].

Herein, in this research, a small amount of NiO was selected to be added in LSCF, because it could tailor the electrode microstructure that leads to improvement in its performance according to a previous study on the anode part of SOFC [11, 12]. NiO has attracted much attention to improve the performance of MIEC. As reported by Czelej et. al, NiO improves the oxygen surface exchange rate because it is highly reactive to the reduction in oxygen when used in the cathode side [13]. NiO also has been reported to have excellent catalytic activity and long-term stability [14]. Most studies regarding Ni focused on the anode side of SOFC due to its low cost, high activity, and stability in reducing the fuel. However, no work has been done to study the effect of NiO addition in the cathode of IT-SOFC. Thus, effect of NiO presence in the cathode side of IT-SOFC and their compatibility with LSCF were done in this work. The active surface area, minimum calcination temperature, dispersion of NiO, crystal size, and polarization resistance of the prepared LSCF-NiO were systematically reported and discussed in the present study.

2. Experimental

2.1. Chemicals and Materials

All materials were in research grade without any further purification. The following materials were used in this study: lanthanum nitrate hexahydrate [$\text{La}(\text{NO}_3)_3 \cdot 6\text{H}_2\text{O}$, MERCK Sdn. Bhd., Malaysia], strontium nitrate hexahydrate [$\text{Sr}(\text{NO}_3)_2$, grade AR, Friendemann Schmidt Chemicals, Germany], cobalt nitrate hexahydrate [$\text{Co}(\text{NO}_3)_2 \cdot 6\text{H}_2\text{O}$, ChemAR, Malaysia], ferum nitrate nonahydrate [$\text{Fe}(\text{NO}_3)_3 \cdot 9\text{H}_2\text{O}$, ChemPur, Malaysia], and nickel nitrate hexahydrate [$\text{Ni}(\text{NO}_3)_2$, R&M Chemical, Malaysia] as the base metal nitrates; citric acid (CA) monohydrate ($\text{C}_6\text{H}_8\text{O}_7 \cdot \text{H}_2\text{O}$, R&M Chemical, Malaysia) as the chelating agent; ethylene glycol (EG, $\text{C}_2\text{H}_6\text{O}_2$, R&M Chemical) as the polymerizing agent; gadolinium-doped cerium (GDC, Sigma–Aldrich, USA) as the electrolyte; ethylcellulose ($\text{C}_{23}\text{H}_{24}\text{N}_6\text{O}_4$, Sigma–Aldrich, Malaysia) and

terpineol (C₁₀H₁₈O, Sigma–Aldrich, Malaysia) as binder; and platinum paste (Sigma–Aldrich, Malaysia) as the current collecting layer.

2.2. Preparation of LSCF-NiO Powder and Symmetrical Cell of LSCF-NiO|GDC|LSCF-NiO

LSCF powder was prepared via modified Pechini method using metal nitrates (M⁺), citric acid (CA), and ethylene glycol (EG) at the ratio of M⁺:CA:EG = 1:4:1. All the materials were dissolved and mixed thoroughly in a fume hood at 100 °C until the solution became a transparent gel. The gel was transferred into silica-alumina crucible and calcined at 600 °C (LSCF 600), 700 °C (LSCF 700), 800 °C (LSCF 800), and 900 °C (LSCF 900), with 100 °C interval for 6 h. The calcined powder was crushed and sieved to produce homogeneous particle size. NiO powder was prepared in a similar fashion by using nickel nitrate hexahydrate and calcined at the same temperature region and profiles. The prepared LSCF powder was then mixed with 5% NiO, and heated at 600 °C (LSCF-NiO 600), 700 °C (LSCF-NiO 700), 800 °C (LSCF-NiO 800), and 900 °C (LSCF-NiO 900). All the LSCF-NiOs were sieved again and stored properly.

The GDC commercial powder was pressed in a 13 mm-diameter mould at 4 MPa for 2 minutes to form a pellet and sintered at 1300 °C for 6 h. Both sides of the sintered pellet were cleaned using 800–1200 sandpaper. Only LSCF-NiO 800 was chosen for the preparation of cathode slurry. Ethyl cellulose and terpineol were thoroughly mixed until they became homogeneous, and then the LSCF-NiO 800 powder was added and continuously mixed to produce fine slurry. By using a brushing technique, a layer of LSCF-NiO 800 was consecutively applied five times on each surface of the GDC pellet, followed by a platinum layer as a current collector to produce a symmetrical cell of LSCF-NiO 800|GDC|LSCF-NiO 800. The fabricated symmetrical cell was sintered at 800 °C for 6 h. A summary of the processing temperature for the preparation of LSCF, NiO, and LSCF-NiO powders is presented in Table 1.

Table 1: Processing temperature for the preparation of LSCF, NiO, and LSCF-NiO powders.

Sample	Processing temperature (°C)	Sample ID
LSCF	600	LSCF 600
	700	LSCF 700
	800	LSCF 800
	900	LSCF 900
LSCF-NiO	600	LSCF-NiO 600
	700	LSCF-NiO 700
	800	LSCF-NiO 800
	900	LSCF-NiO 900

2.3. Sample Characterization

A Fourier-transform infrared (FTIR) spectrometer (Pelkin Elmer) was used to study the presence of functional groups, such as organic, polymeric, and inorganic components, in the samples. The spectrum was collected from 4000⁻¹ to 500 cm⁻¹ at room temperature for the sample in form of a powder. Phase identification of the calcined samples was conducted using X-ray diffraction (XRD, AXS Bruker GmbH) with Cu-K α radiation for 2 θ from 10° to 70°. Bragg's law was applied to confirm the structure of the prepared cathode. The XRD lattice constants a, b, and c were compared to the JCPDS card that generated the highest score in Xpert-Highscore plus during search and match. Perovskite structure percentage and crystal size were calculated using Swarts and Shroust's equation and Scherrer's equation, as given by Eqs. (1) and (2), respectively.

$$\text{Perovskite phase} = \left(\frac{I_p}{I_p - I_m} \right) \times 100\% \quad (1)$$

$$L = \frac{k\lambda}{\beta \cos\theta} \quad (2)$$

where k is shape factor (0.89), λ is the X-ray wavelength (1.54 nm), β is the full width at half maximum (FWHM), and θ is the diffraction angle in radian. A scanning electron microscopy (Quanta FEG 650) with energy dispersive X-ray (EDX) system was used to obtain the microstructures and approximate elemental composition. SEM image analysis software was used to estimate the particle size of the samples and the porosity of a cross section (ImageJ 1.45). The SSA of the cathode powder was measured using the Brunauer–Emmett–Teller (BET) analyzer ASAP 2020 (Micrometrics, USA). Electrochemical impedance spectroscopy (EIS) was adopted (PGSTAT302N, Metrohm Autolab) for electrochemical characterization. Silver wires were attached to the electrodes' platinum paste-coated surfaces. A type-K thermocouple was used to measure the symmetric-cell temperature, which was then recorded using a Digi-Sense digital thermocouple meter (Eutech Instrument). EIS measurement was carried out in the temperature range of 600 °C–800 °C under open-air condition at a frequency range of 0.1 Hz–1 MHz and a signal amplitude of 10 mV. The experimental data were fitted to the equivalent circuit by using Metrohm Autolab NOVA software (version 1.10), with each data plotted using Origin software. The activation energy was calculated using the formula 3 below.

$$K = Ae^{-\frac{E_a}{RT}} \quad (3)$$

where K is the rate, E_a is activation energy, R is the ideal gas constant and T is the temperature.

3. Result and Discussion

3.1. Functional Group Analysis

Figure 1 depicts the Fourier Transform Infra-red (FTIR) spectra of LSCF 600, LSCF 700, LSCF 800, and LSCF gel (precursor state). In the precursor stage, two functional groups, namely, carbonyl and OH, were identified. The presence of carbonyl was expected as CA was used as the chelating agent and it is known the existence of carbonyl bond in citric acid. After the calcination process, small peaks could still be seen in the OH region of the spectrum due to the high humidity percentage of the surrounding air and in the room, which allowed the sample to collect moisture.

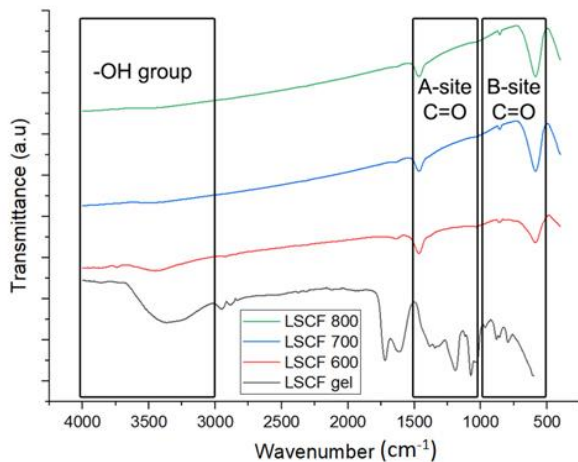


Fig. 1. FTIR spectra of LSCF after calcination at different temperatures according to previous research [15].

The presence of absorption band at 860 and 1460 cm^{-1} for samples LSCF 600, LSCF 700, and LSCF 800 could be associated to the carbonate bonds. The peaks in LSCF gel were substantially higher than those in the other samples due to the presence of OH groups and metal ion interactions. The OH group present due to high air humidity during the sample preparation. The presence of the COO^- complex could not be completely removed even though the calcination temperature was increased to 800 $^{\circ}\text{C}$. This finding indicated that high calcination temperature is required to remove the carbonate group.

As the calcination process was carried out in open air and with the use of organic compound (CA and EG), obtaining a pure sample without carbonate species was difficult. This finding demonstrated the reason for the presence of carbonate group in all samples. Metal oxide bonds could be observed at a wavelength of 560 cm^{-1} . Mani et al. concluded that the peak that appeared between 800 and 500 cm^{-1} was mainly due to metal oxide interaction [16]. Tan et al. reported that the peak between 950 and 500 cm^{-1} was the peak obtained from the B site of the perovskite structure [17]. Thus, these linkages implied the presence of perovskite structure in the samples [18].

3.2. Phase Analysis

The XRD pattern for LSCF-NiO at various calcination temperatures ranging from 600 $^{\circ}\text{C}$ to 900 $^{\circ}\text{C}$ in addition to LSCF and NiO is shown in Fig. 2. LSCF and NiO peaks were labelled with X and #, respectively. Calcination temperature affected the crystallite sizes of LSCF-NiO. In particular, the crystallite size increased as the calcination temperature increased. The entire LSCF-NiO peaks increased and exhibited a narrower shape, indicating an increase in crystallinity [19]. The LSCF powder that was calcined at 600 $^{\circ}\text{C}$ was disqualified from further characterization due to the existence of extra peaks that contributed to the formation of SrCO_3 [20].

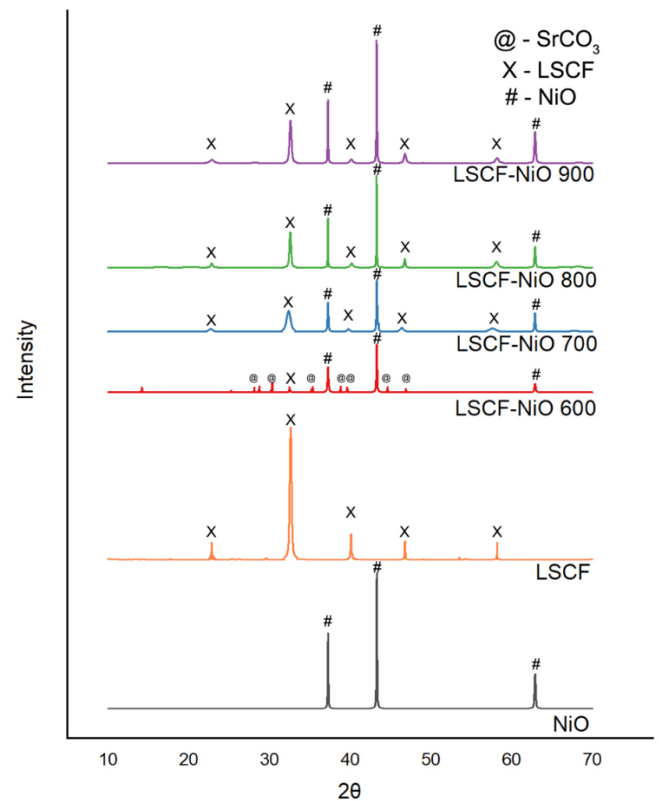


Fig. 2. XRD result comparing LSCF, NiO, and LSCF-NiO at 600 $^{\circ}\text{C}$ –900 $^{\circ}\text{C}$ according to previous research [15].

LSCF-NiO 700, LSCF-NiO 800, and LSCF-NiO 900 showed LSCF and NiO peaks with no secondary phase. This finding indicated that LSCF and NiO have a good chemical affinity with each other and pointed out that the calcination temperature for LSCF-NiO must be at least 700 $^{\circ}\text{C}$. Sun et al. [21] reported that to produce a pure perovskite phase, a minimum calcination temperature of 750 $^{\circ}\text{C}$ is required. In the present study, LSCF perovskite structure could be formed at 700 $^{\circ}\text{C}$. The NiO peaks found matched with JCPDS 78-0643, and the LSCF peaks fit JCPDS 89-1268 (Table 2). The ability to produce a single-phase perovskite structure with no apparent secondary phase revealed that the LSCF and NiO synthesized using a modified method in the present study were suitable.

Table 2. Lattice constant of LSCF and NiO peaks in all samples.

Sample	Peaks	Lattice constant (Å)		
		a	b	c
LSCF-NiO 600	LSCF	5.5169	5.4779	8.1192
	NiO	4.1765		
LSCF-NiO 700	LSCF	5.4996	5.5228	7.8583
	NiO	4.1768		
LSCF-NiO 800	LSCF	5.4991	5.5458	7.8709
	NiO	4.1777		
LSCF-NiO 900	LSCF	5.4934	5.5911	7.8912
	NiO	4.1776		
JCPDS standard	LSCF	5.475	5.536	7.848
	NiO	4.179		

The average crystal size obtained through Scherrer's equation and the perovskite phase percentage obtained using Swarts and Shrou's equation was presented in Table 3. For LSCF-NiO 700, LSCF-NiO 800, and LSCF-NiO 900, a definite trend could be noticed, in which increasing the calcination temperature increased the crystal size and perovskite phase, thus allowing for considerable crystal development. This findings in line with the previous work done by Fatah & Hamid [10].

Table 3. Average crystal size obtained through Scherrer's equation and perovskite phase percentage obtained using Swarts and Shrou's equation.

Sample	Average crystal size (nm)	Perovskite phase (%)
LSCF-NiO 600	57.845	75.49
LSCF-NiO 700	12.129	89.14
LSCF-NiO 800	37.588	96.38
LSCF-NiO 900	50.918	97.85

3.3. Surface Morphology Analysis

SEM analysis was conducted to study the surface morphology and particle size of the samples. Figures 3(a–d) show the SEM images of LSCF-NiO nanoparticles calcined at 600 °C–900 °C at same magnification of 150,000 x. Porous morphology could be observed in all of the samples, in line with other studies that used citrate gel method [18]. The mean diameters of the particles were 97.96, 106.4, 116.2, and 153.3 nm after calcination at

600 °C, 700 °C, 800 °C, and 900 °C, respectively. Close inspection depicted that the particle size was affected by the calcination temperature. LSCF-600 obviously showed the smallest particle size among all samples. The tendency of particle agglomeration became apparent as the temperature exceeded 900 °C, resulting in a substantially bigger particle size. The finding is consistent with the findings of previous studies, in which calcination temperature clearly had a significant effect on powder morphology and facilitated the growth of the particle size of the materials [18, 22–24]. In this regard, the calcination temperature of 700 °C was found to be sufficient to produce LSCF-NiO powder with a minimum average crystal size, as confirmed by XRD analysis (Fig. 2).

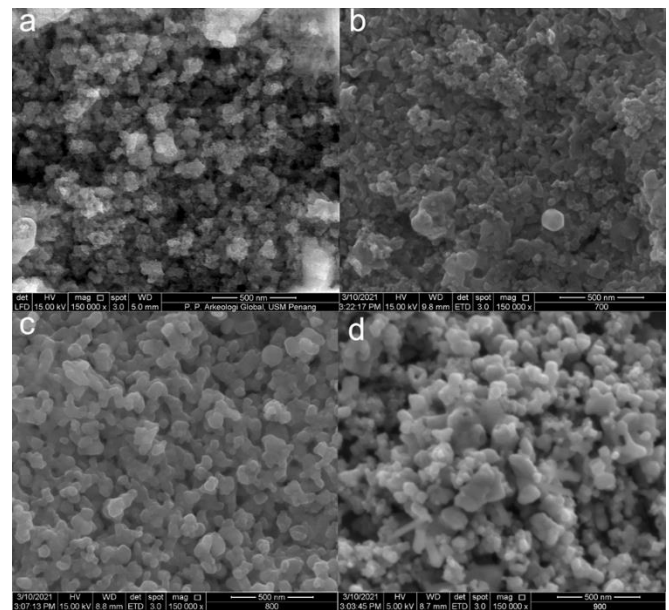


Fig. 3. SEM images of LSCF-NiO prepared at (a) 600 °C, (b) 700 °C, (c) 800 °C, and (d) 900 °C, respectively [15].

The adhesion between the electrolyte and the LSCF-NiO cathode was also investigated using SEM. In general, high sintering temperatures enhanced the adhesion, together with the particle size. They could cause the electrolyte and cathode particles to clump together, thus decreasing the number of active sites for ORR [25]. As such, it is important to find an optimal calcination temperature that produces good particle sizes with good adhesion. A cross section of the electrolyte and LSCF-NiO cathode sintered at 800 °C is shown in Fig. 4. In this case, the cathode powder calcined at 800 °C was used to fabricate the cathode layer by manually brushing the cathode paste onto the SDC electrolyte. The electrolyte and the cathode demonstrated good adhesion without any delamination. Analysis using Image-J software showed that the porosity for the cathode part was approximately 28%, which is in a good range of 20%–40% for the cathode to work properly [26]. This finding suggested that sintering the cell at 800 °C promoted good adhesion between the LSCF-NiO cathode and the electrolyte layer.

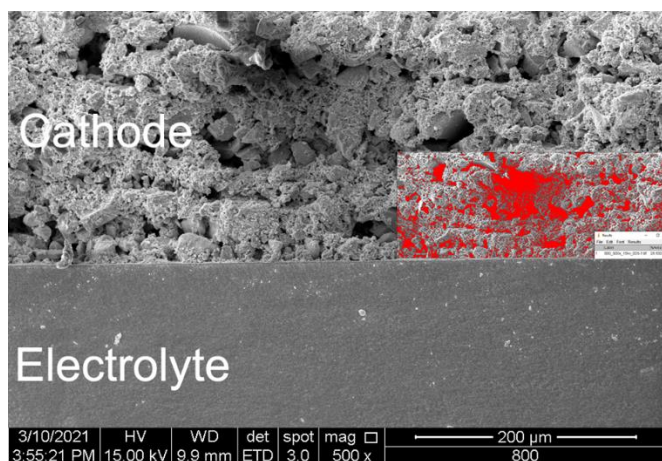


Fig. 4. SEM images of cross section at 500 x magnification between LSCF-NiO 800 cathode and GDC electrolyte (inset is a porosity analysis of the LSCF-NiO 800 cathode).

3.4. Elemental Analysis

By using energy dispersive X-ray (EDX) analysis, a crucial piece of information was obtained, which is the element distribution. Ensuring that the metal element is uniformly spread throughout the surface without the presence of any impurities is crucial to achieve excellent performance. Table 4 summarizes the respective estimation of nominal and experimental stoichiometry of the prepared samples. The site fractions were calculated using LSCF in its pure ABO_3 perovskite phase, including La and Sr on the A sites and Co and Fe on the B sites. The composition of Ni was not included in this evaluation to evaluate the actual composition elements of La, Sr, Co, and Fe in LSCF-NiO compared with the nominal elemental composition in pure LSCF. In all samples, the elemental proportion of La/Sr differed slightly from the nominal fraction. This could occur as a result of the ingredients that could have been lost during the preparation. Another possibility is that Sr segregation phenomenon might happen during the heat treatment process where it was driven to the cathode surface, allowing EDX to identify them rather than other chemicals [27]. However, as the percentage of Sr only increased by 1%–2%, it could not have much effect on the cathode performance.

Figures 5a and b depict the element distribution in LSCF-NiO calcined at 700 °C and 800 °C, respectively. The LSCF-NiO surface layer exhibited a homogeneous distribution of all elements, which were defined as La, Sr, Co, Fe, Ni, and O depending on their distinct colours. Even after sintering at 700 °C and 800 °C, EDX key mapping revealed no evidence of GDC electrolyte, suggesting a good chemical affinity between cathode and electrolyte. Another study also employed a similar technique to display the element distribution in the cathode surface [28–30].

Table 4. EDX data of nominal and experimental stoichiometry for the samples.

Element	La	Sr	Co	Fe
Nominal stoichiometry	0.6	0.4	0.2	0.8
Experimental stoichiometry				
LSCF-NiO 600	0.6	0.4	0.18	0.82
LSCF-NiO 700	0.58	0.42	0.21	0.79
LSCF-NiO 800	0.59	0.41	0.2	0.8
LSCF-NiO 900	0.59	0.41	0.22	0.78

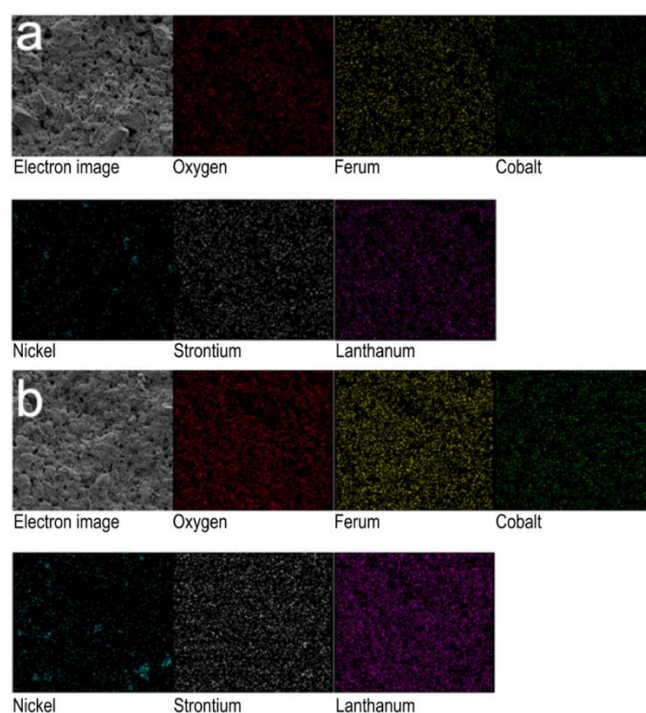


Fig. 5. (a) EDX key mapping for LSCF-NiO 700 °C and (b) 800 °C.

3.5. Surface Area Analysis

Brunauer–Emmett–Teller (BET) analysis was conducted to elucidate the SSA of the LSCF-NiO samples. Cell performance is influenced by factors, such as cathode diffusion ability and the specific surface size (SSA) of the powder. With a high SSA, the TPB is wide, enabling additional oxygen to react. Further cathodic activity could be achieved as more oxygen is converted to O_2^- and transported via the electrolyte, thus improving the overall cell performance [31].

Table 5. Specific surface area and particle size of LSCF-NiO composite cathode material.

Sample	Specific surface area (m ² /g)	Theoretical particle size (nm)	Actual particle size (nm)
LSCF-NiO 600	23.78	51.43	97.96
LSCF-NiO 700	18.29	62.16	106.4
LSCF-NiO 800	7.83	141	116.2
LSCF-NiO 900	6.68	156.55	130.3

Table 5 shows the SSA and its respective theoretical and actual particle sizes. The theoretical particle size (d_{BET}) was calculated by using the actual density obtained from the pycnometer followed by calculation using the following equation [32]:

$$d_{BET} = \frac{6}{S_{BET}} \quad (4)$$

The table clearly indicates that the increase in sintering temperature resulted in an increase in particle size and a decrease in SSA. High temperatures encouraged the particles to stick together to form agglomerates. This pattern is consistent with the results of previous research in a similar field [10]. The sample prepared at 600 °C showed a significantly larger SSA than the other samples calcined at higher temperatures. However, according to XRD, the LSCF perovskite could only be formed at a minimum temperature of 700 °C. The sample calcined 700 °C showed a high SSA of 18.3 m²/g, indicating a suitable powder size for preparing cathode slurry. The sample calcined at 700 °C and 800 °C showed larger SSA than the commercially available bare LSCF (7.7 m²/g) [33] and the LSCF from a previous study (15 m²/g) [16]. This finding indicated that the modified sol-gel method has potential to produce a very fine powder of LSCF-NiO cathode for solid oxide fuel cell application.

The concept that causes large particle size is called grain growth, which is enlargement of grains (crystallites) in a material at high temperatures (Fig. 6a). The fraction of grain boundary atoms increases as the temperature rises. In addition, as the degree of atomic disorder increases, the grain boundary melts, and the density of partial dislocations decreases. Samples at high temperatures have lower resistance to grain growth than those at low temperatures, causing the particle size to grow during high calcination temperature [34].

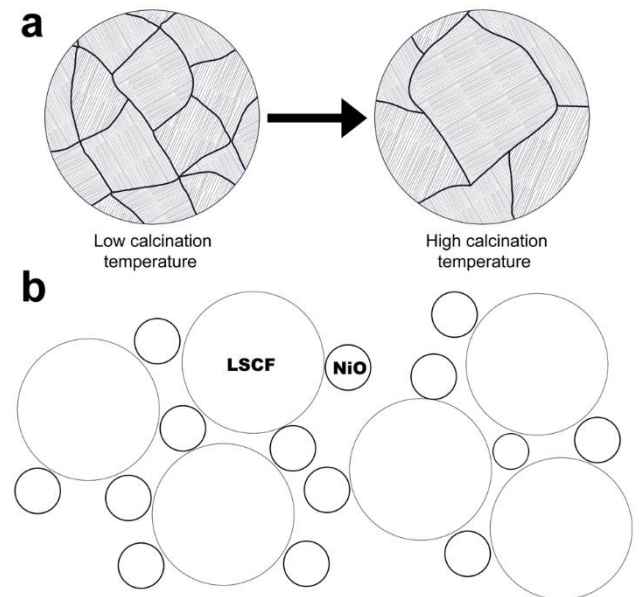


Fig. 6. (a) Grain growth during high temperature and (b) schematic of nickel oxide positioning in LSCF cathode.

A previous study by Zhang et al. [6] suggested that adding metal oxide could enhance SSA because of its smaller particle size than LSCF. The atomic radius of NiO is much smaller than that of LSCF (NiO = 1.69 Å, LSCF = 3.89 Å) [35]. The smaller particle could fill the large void between the LSCF particles, thus enhancing the overall SSA (Fig. 6b). High catalytic activity could be expected from the sample with a large SSA. This result supported that of SEM analysis, which showed that high calcination temperature increased the grain growth and decreased the SSA available for catalytic activities.

3.6. Electrochemical Analysis

3.6.1. Polarization resistance

The analysis was done using electro impedance spectroscopy (EIS). The fitted Nyquist plots of the LSCF-NiO | GDC | LSCF-NiO symmetrical cell are displayed in Z' (actual) versus Z'' (imaginary) in Fig. 7. The cathode was sintered at 800 °C. The EIS spectra depicted the evolution of EIS readings as temperature increased from 600 °C to 800 °C. High frequency (1 MHz–1 kHz), middle frequency (1 kHz–1 Hz), and low frequency (1 kHz–1 Hz) are the three frequency regions in general. High frequency is related to electrolyte response, while intermediate and low frequencies are associated with cathode response, according to the Adler–Lane–Steele model [36]. Figure 7 shows that the EIS spectrum gradually became smaller as the operating temperature increased. This phenomenon signified the dependency of the involved reaction to the operating temperature and proved that the electrochemical reactions were thermally activated processes. A similar trend was also observed in other studies [26, 37]. According to Baharuddin et al. [38] and Mani et al. [16], an increase in temperature increases the conductivity of the cathode and leads to a decrease in R_p .

Furthermore, a high temperature gives additional thermal energy to break the energy barrier, allowing oxygen ions to travel more freely across the electrode and electrolyte [39].

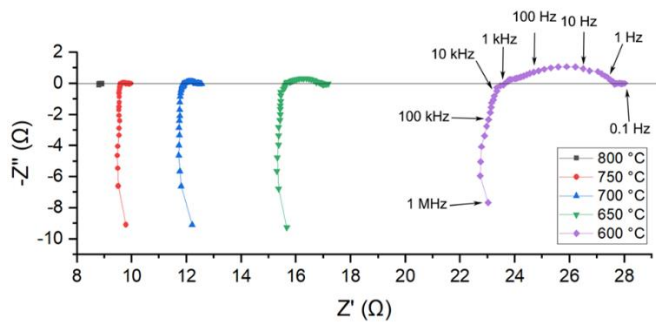


Fig. 7. Impedance spectra of LSCF-NiO tested at 600 °C–800 °C.

Figures 8 (a–e) show the EIS spectrum fitting results at 600 °C–800 °C, with 50 °C interval. The electrolyte resistance of the cell and the inductance impact (at high frequency) were removed from the EIS data to make the polarisation resistance comparison process easy. The impedance spectra in the figure showed two arcs, indicating two electrode reactions. R_s denotes electrolyte resistance, while R_1Q_1 and R_2Q_2 denote the cathode processes in the equivalent circuit of $R_s (R_1Q_1R_2Q_2)$, as shown in Fig. 8. The resistance in the circuit is denoted by R , while the constant phase element (CPE) is denoted by Q . By using the value from the CPE, the associated capacitance (C) and peak arc frequency (f_0) were calculated, as shown in Table 6. As for Figs. 8 (d and e), only R_2 was present as the value of R_1 was too small for the device to detect.

Table 6. Calculated values of resistance, capacitance, and arc frequency.

Operating temperature (°C)	600	650	700	750	800
R_1 (Ω cm ²)	0.55	0.196	0.075		
C_1 (F cm ²)	4.691 $\times 10^{-4}$	9.26 $\times 10^{-4}$	9.26 $\times 10^{-4}$		
f_{01} (Hz)	613	876.4	860.8		
R_2 (Ω cm ²)	3.42	1.04	0.298	0.115	0.021
C_2 (F cm ²)	1.38 $\times 10^{-2}$	1.14 $\times 10^{-2}$	1.09 $\times 10^{-2}$	1.47 $\times 10^{-2}$	1.86 $\times 10^{-2}$
f_{02} (Hz)	3.37	12.9	48.9	94.1	408.9

By using the capacitance values obtained from the calculation based on the fitting results, the cathode response was allocated under the EIS spectrum. The dotted line in Figs. 8 (a–e) denotes the response resolved from the EIS result.

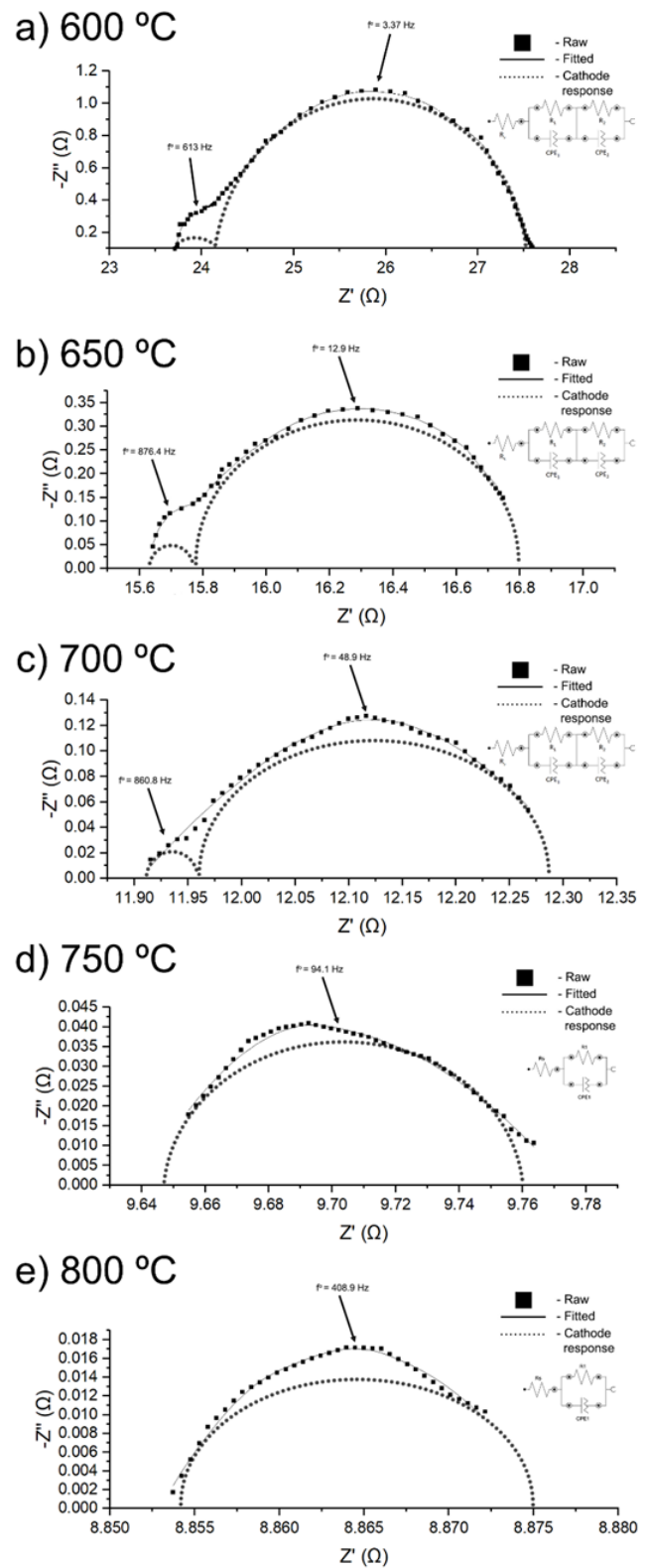


Fig. 8. EIS spectra of LSCF-NiO 800 | GDC | LSCF-NiO 800 tested at (a) 600 °C, (b) 650 °C, (c) 700 °C, (d) 750 °C, and (e) 800 °C (Inset is an equivalent circuit at the respective temperature).

The value of capacitance in Table 6 serves as the identification of the reaction occur at that point. The capacitance value at the first arc (R_1Q_1) was in the range of $C \approx 10^{-4}$ – 10^{-3} Fcm², suggesting the contribution of ionic charge transfer at the

cathode/electrolyte interface. Meanwhile, the second arc R_2Q_2 indicates the adsorption/dissociation on the cathode surface and diffusion of oxygen as it has a value of capacitance at $C \approx 10^{-2} \text{ Fcm}^2$ [40].

Polarization resistance refers to the summation of R_1 and R_2 . A previous study by Jiang [41] reported that the conventional LSCF had the R_p of $1.3 \Omega \text{ cm}^2$ when it was operated at $700 \text{ }^\circ\text{C}$. In this study, the R_p of LSCF-NiO was only $0.37 \Omega \text{ cm}^2$. In 2015, Lourerio et al. [42] reported that that LSCF-SDC performed better than the LSCF counterpart at $750 \text{ }^\circ\text{C}$, which showed an R_p of $0.33 \Omega \text{ cm}^2$. Considering that the present study showed that an R_p of $0.12 \Omega \text{ cm}^2$ at the same operating temperature, it can be said that LSCF-NiO is also performed better than LSCF. The results proved that LSCF-NiO sintered at $800 \text{ }^\circ\text{C}$ is acceptable as a cathode candidate for IT-SOFCs, as the previous study suggested that a good cathode requires an R_p of less than $1 \Omega \text{ cm}^2$ [43].

3.6.2. Activation energy

The activation energy of LSCF-NiO was determined using the Arrhenius plot, as shown in Fig. 9. The LSCF-NiO electrode's activation energy was found to be 1.65 eV or 159.5 kJ/mol . The pristine conventional LSCF, according to Xi et al. (2016), had a higher E_a of 186 kJ/mol [30]. Garcia et al. [44] investigated the effect of sintering temperature on the E_a of a cathode sintered at various temperatures. The LSCF sintered at $1200 \text{ }^\circ\text{C}$ had an E_a of 157.8 kJ/mol . In conjunction to the activation energy of conventional LSCF, the addition of NiO can lower the activation energy by $\sim 26.5 \text{ kJ/mol}$. This finding proved that NiO has a capability of enhancing the ORR process, which lowers the overall polarization resistance of the cathode. Even though the sintering temperature reduced by $400 \text{ }^\circ\text{C}$ in the present work, LSCF-NiO displayed a similar E_a , demonstrating the ability of NiO to accomplish the equivalent result at lower temperatures.

4. Conclusion

In this study, addition of NiO to produce LSCF-NiO composite cathode powder shows low agglomeration, small crystallite size and high BET specific surface area. FTIR result suggested that the existence of metal bonds along with carbonate bonds in all composite cathode samples. The EIS result proved that the LSCF-NiO sample is fit to be used at intermediate temperature with low enough polarization resistance. The composite cathode of LSCF-NiO presented in this study showed a lower E_a value compared to that of conventional LSCF cathode, proving that the addition of NiO can lower the

E_a . Overall, LSCF-NiO is a potential composite cathode for application in intermediate temperature SOFCs and can be used as an alternative cathode to replace conventional LSCF cathode.

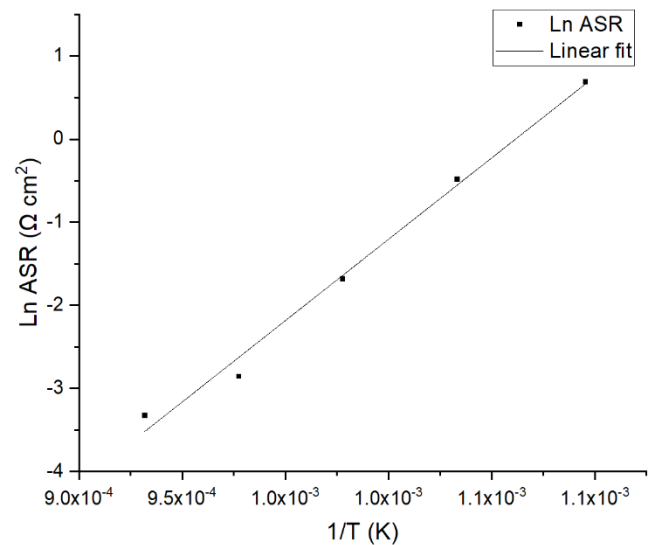


Fig. 9. Arrhenius plot for LSCF-NiO sintered at $800 \text{ }^\circ\text{C}$.

Acknowledgement

The authors wish to acknowledge the financial support from by the RUI grant provided by Universiti Sains Malaysia (1001/PJKIMIA/8014139) and the collective research support provided by Universiti Teknologi MARA and Universiti Kebangsaan Malaysia.

References

- [1] S. Burnwal, S. Bharadwaj, and P. Kistaiah, "Review on MIEC cathode materials for solid oxide fuel cells," *Journal of Molecular and Engineering Materials*, vol. 4, no. 2, p. 1630001, 2016, doi: 10.1142/S2251237316300011.
- [2] L. Lu, Q. Shi, Y. Yang, and H. Zhang, "Electrochemical performance of $(\text{La,Sr})(\text{Co,Fe})\text{O}_{3-\delta}-(\text{Ce,Sm})\text{O}_{2-\theta}-\text{CuO}$ composite cathodes for intermediate temperature solid oxide fuel cells," *Materials Research Bulletin*, vol. 47, no. 4, pp. 1016-1020, 2012, doi: <https://doi.org/10.1016/j.materresbull.2012.01.005>.
- [3] T. E. Burye and J. D. Nicholas, "Nano-ceria pre-infiltration improves $\text{La}_{0.6}\text{Sr}_{0.4}\text{Co}_{0.8}\text{Fe}_{0.2}\text{O}_{3-x}$ infiltrated solid oxide fuel cell cathode performance," *Journal of Power Sources*, vol. 300, pp. 402-412, 2015, doi: <https://doi.org/10.1016/j.jpowsour.2015.09.080>.
- [4] H. J. Hwang, J.-W. Moon, S. Lee, and E. A. Lee, "Electrochemical performance of LSCF-based composite cathodes for intermediate temperature SOFCs," *Journal of Power Sources*, vol. 145, no. 2, pp. 243-248, 2005, doi: <https://doi.org/10.1016/j.jpowsour.2005.02.063>.

- [5] A. J. Abd Aziz, N. A. Baharuddin, M. R. Somalu, and A. Muchtar, "Review of composite cathodes for intermediate-temperature solid oxide fuel cell applications," *Ceramics International*, vol. 46, no. 15, pp. 23314-23325, 2020, doi: 10.1016/j.ceramint.2020.06.176.
- [6] L. Zhang, T. Hong, Y. Li, and C. Xia, "CaO effect on the electrochemical performance of lanthanum strontium cobalt ferrite cathode for intermediate-temperature solid oxide fuel cell," *International Journal of Hydrogen Energy*, vol. 42, no. 27, pp. 17242-17250, 2017, doi: 10.1016/j.ijhydene.2017.05.207.
- [7] M. Nadeem, B. Hu, and C. Xia, "Effect of NiO addition on oxygen reduction reaction at lanthanum strontium cobalt ferrite cathode for solid oxide fuel cell," *International Journal of Hydrogen Energy*, vol. 43, no. 16, pp. 8079-8087, 2018, doi: 10.1016/j.ijhydene.2018.03.053.
- [8] Y. Yang, M. Li, Y. Ren, Y. Li, and C. Xia, "Magnesium oxide as synergistic catalyst for oxygen reduction reaction on strontium doped lanthanum cobalt ferrite," *International Journal of Hydrogen Energy*, vol. 43, no. 7, pp. 3797-3802, 2018/02/15/ 2018, doi: <https://doi.org/10.1016/j.ijhydene.2017.12.183>.
- [9] A. F. Mohd Abd Fatah, M. N. Murat, and N. A. Hamid, "LSCF-CuO as promising cathode for it sofc," *Journal of Engineering and Technological Sciences*, vol. 53, no. 4, 2021, Art no. 210411, doi: 10.5614/j.eng.technol.sci.2021.53.4.11.
- [10] A. F. Fatah and N. A. Hamid, "Physical and chemical properties of LSCF-CuO as potential cathode for intermediate temperature solid oxide fuel cell (IT-SOFC).pdf," *Malaysian Journal of Fundamental and Applied Sciences*, 2018, doi: 10.11113/mjfas.v14n3.1220.
- [11] I. Hwang, J. Jeong, K. Lim, and J. Jung, "Microstructural characterization of spray-dried NiO-8YSZ particles as plasma sprayable anode materials for metal-supported solid oxide fuel cell," *Ceramics International*, vol. 43, no. 10, pp. 7728-7735, 2017/07/01/ 2017, doi: <https://doi.org/10.1016/j.ceramint.2017.03.077>.
- [12] Z. Liu, X. Wang, M. Liu, and J. Liu, "Enhancing sinterability and electrochemical properties of Ba(Zr_{0.1}Ce_{0.7}Y_{0.2})O_{3-δ} proton conducting electrolyte for solid oxide fuel cells by addition of NiO," *International Journal of Hydrogen Energy*, vol. 43, no. 29, pp. 13501-13511, 2018, doi: 10.1016/j.ijhydene.2018.05.089.
- [13] K. Czelej, K. Cwieka, J. C. Colmenares, and K. J. Kurzydowski, "Catalytic activity of NiO cathode in molten carbonate fuel cells," *Applied Catalysis B: Environmental*, vol. 222, pp. 73-75, 2018, doi: <https://doi.org/10.1016/j.apcatb.2017.10.003>.
- [14] M. B. Askari, P. Salarizadeh, M. Seifi, and S. M. Rozati, "Ni/NiO coated on multi-walled carbon nanotubes as a promising electrode for methanol electro-oxidation reaction in direct methanol fuel cell," *Solid State Sciences*, vol. 97, p. 106012, 2019, doi: <https://doi.org/10.1016/j.solidstatedsciences.2019.106012>.
- [15] A. Z. Rosli, M. R. Somalu, N. Osman, and N. A. Hamid, "Physical characterization of LSCF-NiO as cathode material for intermediate temperature solid oxide fuel cell (IT-SOFCs)," *Materials Today: Proceedings*, vol. 46, pp. 1895-1900, 2021, doi: 10.1016/j.matpr.2021.01.778.
- [16] R. Mani, R. K. Gautam, S. Banerjee, A. K. Srivastava, A. Jaiswal, and M. C. Chattopadhyaya, "A study on La_{0.6}Sr_{0.4}Co_{0.3}Fe_{0.8}O₃(LSCF) cathode material prepared by gel combustion method for IT-SOFCs: spectroscopic, electrochemical and microstructural analysis," *Asian Journal of Research in Chemistry*, vol. 8, no. 6, 2015, doi: 10.5958/0974-4150.2015.00062.0.
- [17] K. H. Tan, H. A. Rahman, and H. Taib, "Ba_{0.5}Sr_{0.5}Co_{0.8}Fe_{0.2}O_{3-δ}-Sm_{0.2}Ce_{0.8}O_{1.9} carbonate perovskite coating on ferritic stainless steel interconnect for low temperature solid oxide fuel cells," *Materials Chemistry and Physics*, vol. 254, 2020, doi: 10.1016/j.matchemphys.2020.123433.
- [18] W.-D. Yang, Y.-H. Chang, and S.-H. Huang, "Influence of molar ratio of citric acid to metal ions on preparation of La_{0.67}Sr_{0.33}MnO₃ materials via polymerizable complex process," *Journal of the European Ceramic Society*, vol. 25, no. 16, pp. 3611-3618, 2005, doi: 10.1016/j.jeurceramsoc.2004.09.028.
- [19] B. Habibi and S. Ghaderi, "Electrooxidation of formic acid and formaldehyde on the Fe₃O₄@Pt core-shell nanoparticles /carbon-ceramic electrode," *Iranian Journal of Chemistry and Chemical Engineering*, vol. 35, pp. 99-112, 12/01 2016. doi: 10.1016/j.ssi.2016.11.008.
- [20] L. da Conceição, A. M. Silva, N. F. P. Ribeiro, and M. M. V. M. Souza, "Combustion synthesis of La_{0.7}Sr_{0.3}Co_{0.5}Fe_{0.5}O₃ (LSCF) porous materials for application as cathode in IT-SOFC," *Materials Research Bulletin*, vol. 46, no. 2, pp. 308-314, 2011, doi: 10.1016/j.materresbull.2010.10.009.
- [21] Y. Sun, N. Yan, J. Li, H. Wu, J.-L. Luo, and K. T. Chuang, "The effect of calcination temperature on the electrochemical properties of La_{0.3}Sr_{0.7}Fe_{0.7}Cr_{0.3}O_{3-x} (LSFC) perovskite oxide anode of solid oxide fuel cells (SOFCs)," *Sustainable Energy Technologies and Assessments*, vol. 8, pp. 92-98, 2014, doi: doi.org/10.1016/j.seta.2014.08.001.
- [22] L. Abdul Malik *et al.*, "Effect of nickel oxide - Modified BaCe_{0.54}Zr_{0.36}Y_{0.1}O_{2.95} as composite anode on the performance of proton-conducting solid oxide fuel cell," *International Journal of Hydrogen Energy*, vol. 46, no. 8, pp. 5963-5974, 2021, doi: 10.1016/j.ijhydene.2020.10.219.
- [23] S. L. Zhang, Y. B. Shang, C. X. Li, and C. J. Li, "Vacuum cold sprayed nanostructured La_{0.6}Sr_{0.4}Co_{0.2}Fe_{0.8}O_{3-δ} as a high-performance cathode for porous metal-supported solid oxide fuel cells operating below 600 °C," *Materials Today Energy*,

- vol. 21, p. 100815, 2021, doi: <https://doi.org/10.1016/j.mtener.2021.100815>.
- [24] L. Liu, Z. Zhang, S. Das, S. Xi, and S. Kawi, "LaNiO₃ as a precursor of Ni/La₂O₃ for reverse water-gas shift in DBD plasma: Effect of calcination temperature," *Energy Conversion and Management*, vol. 206, p. 112475, 2020, doi: <https://doi.org/10.1016/j.enconman.2020.112475>.
- [25] D. Szymczewska, J. Karczewski, A. Chrzan, and P. Jasinski, "CGO as a barrier layer between LSCF electrodes and YSZ electrolyte fabricated by spray pyrolysis for solid oxide fuel cells," *Solid State Ionics*, vol. 302, pp. 113-117, 2017, doi: [10.1016/j.ssi.2016.11.008](https://doi.org/10.1016/j.ssi.2016.11.008).
- [26] N. A. Baharuddin, A. Muchtar, M. Somalu, M. A, and H. Abd. Rahman, "Influence of sintering temperature on the polarization resistance of La_{0.20}Sr_{0.6}O_{2.0}Co_{0.2}Fe_{0.2}O_{3-δ} - SDC carbonate composite cathode," *Ceramics - Silikaty*, pp. 1-9, 2016, doi: [10.13168/cs.2016.0017](https://doi.org/10.13168/cs.2016.0017).
- [27] B. Koo, K. Kim, J. K. Kim, H. Kwon, J. W. Han, and W. Jung, "Sr Segregation in Perovskite Oxides: Why it happens and how it exists," *Joule*, vol. 2, no. 8, pp. 1476-1499, 2018, doi: <https://doi.org/10.1016/j.joule.2018.07.016>.
- [28] J. Laurencin *et al.*, "Degradation mechanism of La_{0.6}Sr_{0.4}Co_{0.2}Fe_{0.8}O_{3-δ}/Gd_{0.1}Ce_{0.9}O_{2-δ} composite electrode operated under solid oxide electrolysis and fuel cell conditions," *Electrochimica Acta*, vol. 241, pp. 459-476, 2017, doi: <https://doi.org/10.1016/j.electacta.2017.05.011>.
- [29] W.-J. Shong, C.-K. Liu, C.-W. Lu, S.-H. Wu, and R.-Y. Lee, "Characteristics of La_{0.6}Sr_{0.4}Co_{0.2}Fe_{0.8}O₃-Cu₂O mixture as a contact material in SOFC stacks," *International Journal of Hydrogen Energy*, vol. 42, no. 2, pp. 1170-1180, 2017, doi: [10.1016/j.ijhydene.2016.08.211](https://doi.org/10.1016/j.ijhydene.2016.08.211).
- [30] X. Xi, A. Kondo, and M. Naito, "A simple mechanical process to synthesize La_{0.6}Sr_{0.4}Co_{0.2}Fe_{0.8}O₃ perovskite for solid oxide fuel cells cathode," *Materials Letters*, vol. 145, pp. 212-215, 2015, doi: [10.1016/j.matlet.2015.01.116](https://doi.org/10.1016/j.matlet.2015.01.116).
- [31] H. A. Rahman, A. Muchtar, N. Muhamad, and H. Abdullah, "La_{0.6}Sr_{0.4}Co_{0.2}Fe_{0.8}O_{3-δ}-SDC carbonate composite cathodes for low-temperature solid oxide fuel cells," *Materials Chemistry and Physics*, vol. 141, no. 2-3, pp. 752-757, 2013, doi: [10.1016/j.matchemphys.2013.05.071](https://doi.org/10.1016/j.matchemphys.2013.05.071).
- [32] G. Thiele, M. Poston, and R. Brown, "A case study in sizing nanoparticles," Micromeritics Analytical Services, 2007, doi: [10.1515/9783110893915.1](https://doi.org/10.1515/9783110893915.1).
- [33] M. Zawadzki, H. Grabowska, and J. Trawczyński, "Effect of synthesis method of LSCF perovskite on its catalytic properties for phenol methylation," *Solid State Ionics*, vol. 181, no. 23-24, pp. 1131-1139, 2010, doi: [10.1016/j.ssi.2010.06.009](https://doi.org/10.1016/j.ssi.2010.06.009).
- [34] X. Lu *et al.*, "Effects of grain size and temperature on mechanical properties of nano-polycrystalline Nickel-cobalt alloy," *Journal of Materials Research and Technology*, vol. 9, no. 6, pp. 13161-13173, 2020, doi: <https://doi.org/10.1016/j.jmrt.2020.09.060>.
- [35] F. Shen and K. Lu, "La_{0.6}Sr_{0.4}Co_{0.2}Fe_{0.8}O₃ cathodes incorporated with Sm_{0.2}Ce_{0.8}O₂ by three different methods for solid oxide fuel cells," *Journal of Power Sources*, vol. 296, pp. 318-326, 2015, doi: <https://doi.org/10.1016/j.jpowsour.2015.07.060>.
- [36] S. B. Adler, "Limitations of charge-transfer models for mixed-conducting oxygen," *Solid State Ionics*, vol. 135, no. 1-4, pp. 603-612, 2000. doi: [10.1016/S0167-2738\(00\)00423-9](https://doi.org/10.1016/S0167-2738(00)00423-9).
- [37] S. A. Muhammed Ali, M. Anwar, M. R. Somalu, and A. Muchtar, "Enhancement of the interfacial polarization resistance of La_{0.6}Sr_{0.4}Co_{0.2}Fe_{0.8}O_{3-δ} cathode by microwave-assisted combustion method," *Ceramics International*, vol. 43, no. 5, pp. 4647-4654, 2017, doi: <https://doi.org/10.1016/j.ceramint.2016.12.136>.
- [38] N. A. Baharuddin, A. Muchtar, M. R. Somalu, N. S. Kalib, and N. F. Raduwan, "Synthesis and characterization of cobalt-free SrFe_{0.8}Ti_{0.2}O_{3-δ} cathode powders synthesized through combustion method for solid oxide fuel cells," *International Journal of Hydrogen Energy*, vol. 44, no. 58, pp. 30682-30691, 2019, doi: <https://doi.org/10.1016/j.ijhydene.2018.11.142>.
- [39] S. Mohd Senari, N. Osman, and A. M. Md Jani, "Characterization of nio-bczy composite anode prepared by one-step sol-gel method," *Solid State Science and Technology*, vol. 25, no. 1, pp. 135-141, 2018, doi: [10.11113/mjfas.v16n4.1929](https://doi.org/10.11113/mjfas.v16n4.1929).
- [40] I. Ismail, N. Osman, and A. M. M. Jani, "La_{0.6}Sr_{0.4}Co_{0.2}Fe_{0.8}O_{3-δ} powder: A simple microstructure modification strategy for enhanced cathode electrochemical performance," *Journal of Sol-Gel Science and Technology*, vol. 94, no. 2, pp. 435-447, 2020, doi: [10.1007/s10971-020-05231-0](https://doi.org/10.1007/s10971-020-05231-0).
- [41] S. P. Jiang, "Development of lanthanum strontium cobalt ferrite perovskite electrodes of solid oxide fuel cells - A review," *International Journal of Hydrogen Energy*, vol. 44, no. 14, pp. 7448-7493, 2019, doi: [10.1016/j.ijhydene.2019.01.212](https://doi.org/10.1016/j.ijhydene.2019.01.212).
- [42] F. J. A. Loureiro *et al.*, "Cathodic polarisation of composite LSCF-SDC IT-SOFC electrode synthesised by one-step microwave self-assisted combustion," *Journal of the European Ceramic Society*, vol. 39, no. 5, pp. 1846-1853, 2019, doi: [10.1016/j.jeurceramsoc.2019.01.013](https://doi.org/10.1016/j.jeurceramsoc.2019.01.013).
- [43] M. A. S. A, M. Anwar, N. F. Raduwan, A. Muchtar, and M. R. Somalu, "Optical, mechanical and electrical properties of LSCF-SDC composite cathode prepared by sol-gel assisted rotary evaporation technique," *Journal of Sol-Gel Science and Technology*, vol. 86, no. 2, pp. 493-504, 2018, doi: [10.1007/s10971-018-4636-8](https://doi.org/10.1007/s10971-018-4636-8).
- [44] L. M. P. Garcia, D. A. Macedo, G. L. Souza, F. V. Motta, C. A. Paskocimas, and R. M. Nascimento, "Citrate-hydrothermal synthesis, structure and electrochemical performance of



Fuel Cell.

Ahmad Zaki Mohamed Rosli was born in Johor, Malaysia in 1996. He obtained his B.Eng in chemical engineering in 2019 and M.Sc. in a similar field in 2022, both at Universiti Sains Malaysia, Nibong Tebal, Penang, Malaysia.

He worked as a research assistant in Universiti Sains Malaysia for half a year, prior to continuing his Master's degree. He published a research article in *Materials Today: Proceeding* on 2021. His project focuses on cathode for intermediate temperature solid oxide fuel cells. His project was awarded gold medallist in The International Innovation Creativity & Technology Exhibition i2CreaTE 2021, with project title: Composite Cathode for Intermediate Temperature Solid Oxide



Nafisah Osman is a Professor at the Department of Physics, Faculty of Applied Sciences, Universiti Teknologi MARA (UiTM). She completed her Ph.D. at Universiti Kebangsaan Malaysia (UKM) in 2010 and her MSc as well as undergraduate studies at the same university in 2002 and 1990, respectively.

She leads the Physics and Chemistry Materials Research Group (PCMaG) and Proton Conducting Fuel Cell Research Group (PCFCRG) in UiTM. Her works have been internationally and nationally cited, and the number of her citation based on google scholar is about 441 with an h-index of 10. She has graduated 10 postgraduate students, and currently, she supervises 5 Ph.D. students and 5 Master's students. At the national level, she has been a Secretary of the Malaysian Solid State Science Technology and Society (MASS) from 2016-present and a member of the Malaysian Association of Hydrogen Energy (MAHE) from 2017-present. Her research interests lie in advanced materials, solid-state ionic, and materials chemistry. In a recent study, she has focused on better techniques for synthesizing ceramics compounds at relatively low temperatures and fabricating anode-supported single cells with various pure and composite materials of cathode and anode.



Mahendra Rao Somalu received the Bachelor of Engineering (Chemical) in Universiti Kebangsaan Malaysia in 2004, and the Master of Engineering (Chemical) in the same university in 2006. Then, he finished his Ph.D. in 2012 at Imperial College London in the field of fuel cell under the supervision of Prof. Dr. Nigel P. Brandon. Currently, he is an Assoc. Professor at Universiti Kebangsaan Malaysia.

His field of expertise is fuel cell, gasification, nanomaterials and hydrogen energy. He is an associate member of the Institution of Chemical Engineers (IChemE), a member of The Malaysia Association of Hydrogen Energy (MAHE), and a member of The Malaysian Solid State Science and Technology (MASS).

Associate Prof. Dr. Mahendra was awarded Gold Award in the 4th International Malaysia-Indonesia-Thailand Symposium on Innovation and Creativity 2021 (SIC 2021), Anugerah Bitara Penerbitan Makalah Sains, Teknologi dan Kejuruteraan dari Universiti Kebangsaan Malaysia in 2018, Silver Award in the 3rd International Innovation, Design and Articulation (i-IDEA 2016) and Gold Award in the Invention, Innovation & Design Exposition 2015 (iideX2015).



Noorashrina A Hamid was born and raised in Malaysia. She completed her the B.Eng. in Universiti Teknologi Malaysia in 2003 and M.Sc. degrees Universiti Kebangsaan Malaysia in 2009. She furthered her studies in Duisburg-Essen in Germany for her Ph.D. and received her doctorate in 2013.

Currently, she is a senior lecturer in Universiti Sains Malaysia in Nibong Tebal engineering campus in Penang, Malaysia. Her field of expertise is in the energy storage system, electrochemistry, nanotechnology and nanomaterials from conventional as well as aerosol technology. In 2012, she published a research article in the *Journal of Power Sources* entitled 'High-Capacity Cathodes for Lithium-Ion Batteries from Nanostructured LiFePO₄ Synthesized by Highly-Flexible and Scalable Flame Spray Pyrolysis', and won the best paper award 2012 by Centre for Nano Integration Duisburg-Essen (CENIDE). She was awarded a Professional Engineer (Ir.) certificate for her merit in the academic field in 2018.

Appendix

The materials used were Lanthanum nitrate hexahydrate ($\text{La}(\text{NO}_3)_3 \cdot 6\text{H}_2\text{O}$, CAS, 10277-43-7 Acros Organic), Strontium Nitrate ($\text{Sr}(\text{NO}_3)_2$, CAS, 10042-76-9, Friendemann Schmidt), Cobalt Nitrate-hexahydrate ($\text{Co}(\text{NO}_3)_2 \cdot 6\text{H}_2\text{O}$, CAS, 10141-05-6, System), Ferum Nitrate-nonahydrate ($\text{Fe}(\text{NO}_3)_3 \cdot 9\text{H}_2\text{O}$, CAS, 7782-61-8, ACS Reagent), citric acid monohydrate ($\text{C}_6\text{H}_8\text{O}_7 \cdot \text{H}_2\text{O}$, CAS, 77-92-9, RnM Chemical), ethylene glycol ($\text{C}_2\text{H}_6\text{O}_2$, CAS 107-21-1, RnM Chemical) and Gadolinium doped Ceria (GDC) ($\text{Gd}_{0.1}\text{Ce}_{0.9}\text{O}_{1.9}$, Sigma Aldrich) without any purification.